Proceedings of the 7th World Congress on Civil, Structural, and Environmental Engineering (CSEE'22)
~~Lisbon, Portugal~~ Virtual Conference – April 10 – 12, 2022
Paper No. ICGRE 189
DOI: 10.11159/icgre22.189

Waterflow Stochastic Analysis in Fractured Rock Mass

Pedro Baena de Mesquita[1], Leandro Lima Rasmussen[2]
[1]University of Brasília
Campus Universitário Darcy Ribeiro, Asa Norte, Brasília, Brazil
190140593@aluno.unb.br; leandro.lima@unb.br
[2]University of Brasília
Campus Universitário Darcy Ribeiro, Asa Norte, Brasília, Brazil

Abstract **–** Rock masses are often present with numerous discontinuities due to their geological history. These increase the permeability of the rock and facilitate water flow. Nonetheless, water pressure may cause significant stability problems for many underground engineering works. Furthermore, the difficulties in collecting data on the position and the physical properties of the discontinuities present a challenge to understanding the medium behavior. For this purpose, many models may be used to represent the rock mass. Among these, there is the Discrete Fracture Networks. It is a useful tool to represent the discontinuities in the fractured rock mass and for statistical analysis when combined with multiple simulations. Therefore, a new computational code was created that calculated the water flow for a two-dimensional mesh, using the cubic law. Two scenarios were established for the Monte Seco tunnel: the first with a constant hydraulic aperture and the second a hydraulic aperture following a lognormal distribution. It was possible to identify how the water flow is affected by the connectivity of the mesh, especially by the longest fractures sets, and by the hydraulic aperture variability. However, it was not possible to establish a relationship between the water flow and the discontinuities density. Finally, some directions that were more favourable to the insertions of drains were identified. This could help to understand some of the main features of the discontinuities networks that contribute to the water flow and to make some decisions to mitigate the problems associated with it.

Keywords**:** 4 - DFN, water flow, fractured rock mass, statistical analysis, P criteria, drains

1. Introduction

Through their geologic history, fractured rock masses are submitted to stresses that caused the appearance of discontinuities. These create preferential flow paths through the rock matrix, generally less permeable [1]. Water flow through the discontinuities may cause several stability problems during excavations in fractured rock masses for underground works of engineering [2].

Knowing how the water flows through the rock mass may help to make better decisions and to mitigate the negative effects. However, it is normally very hard to obtain trusted parameters of the discontinuities' geometric properties because of little accessibility and the difficulty to collect the data [3]. Therefore, a statistical analysis of the data is an important tool to study the water flux through the fractured rock mass [4].

There are many parameters that regulate the water flux, among which are the geometric properties and the hydraulic aperture of the discontinuities [5]. To understand how each one of them influences water flow is a difficult task [4]. For this reason, the purpose of this article is to analyze how the geometric properties and the density fracture criterion of the rock mass determine water flow and how they may help to choose drains orientation.

2. Literature Review

Many parameters are necessary to characterize the discontinuities. The most important are orientation, the number of joints sets, persistence, among others [5]. Dershowitz and Einstein [6] cite many models that may be used to represent the discontinuities in a fractured rock mass: the orthogonal model, the Baecher model, the Veneziano model, among others.

However, data collection to completely describe the discontinuities poses challenges to its acquisition [3]. The discrete fracture network model enables the representation of the attributes of the discontinuities, position, orientation, persistence, among others, in a simple way, in addition to the use of statistical analyses by means of multiple simulation [2]. The stochastic representation of hydrogeological problems may provide important tools to solve the problem of medium uncertainty [4]. After that the water flux is found by calculating the equilibrium of water incoming and outcoming at the nodes following

Darcy's law. The model assumes that the discontinuities may be simulated as parallel plates [5]. Furthermore, an important element to assess water flux are the flow paths, formed at the intersection of different discontinuities and the connectivity of the mesh.

Reeves et al. [1] analysed many different geometries of hypothetical fractured rock masses, whose trace length followed a power law distribution. They associated the parameter "a", that characterizes the length of the discontinuities, with the mesh density and the output flow rate. They noted that the latter diminished with the increase of the parameter "a". Zhu et al. [7] made a similar observation, as the increase in parameter "a" induced a proportionally greater flow through the rock matrix. The correlation between the transmissivity and the discontinuities' length may be an important one. Reeves et al. [1] obtained a smaller water flux for a variable uncorrelated transmissivity. However, Zhu et al. [7] observed a higher water flux for variable correlated hydraulic aperture. Reeves et al. [1] described three groups of discontinuities: all the discontinuities, hydraulic backbone, discontinuities with at least some water flow, and the dominant discontinuities, the ones responsible for the most part of the water flow. They proposed a model to identify the mean drain length require to intersect a major discontinuity. From that they noted that mean drain length is affected by the discontinuities orientation unless they are randomly oriented. The incorporation of a standard deviation into the transmissivity increased the necessary length to intersect a dominant discontinuity.

However, there are many types of discontinuities, whose trace length does not follow a power law. Therefore, to assess the intensity of fracturation of a rock mass, the P system of Dershowitz and Herda may be used [8]. Their proposition includes many criteria to evaluate for one, two or three dimensions and may be used for any rock mass. In one dimension, the number of discontinuities is evaluated by the number of discontinuities intersecting per length of the study line. For two dimensions, it could be the number of discontinuities per area or their length per area. This is often used to describe the fracture intensity from a trace. Finally, in three dimensions, the number of discontinuities, the sum of the lengths of the discontinuities or the sum of the areas of the discontinuities inside a volume can be used.

The complexity of water flux through the rock mass is reflected in the lack of a unified drain design method [9]. The consideration of the geometry of the discontinuities is essential for the drains to be arranged as efficiently as possible [1]. However, the holes are generally made with the same spacing and the same length, which makes them inefficient [10].

3. Methodology

The methodology adopted in this work is based on Reeves et al. [1]. They found a relationship between the parameter "a" and the water flow and between the parameter "a" and the P21 density criterion. Since not every discontinuity network follows a power law distribution, it was adapted to analyse a possible relation of the waterflow to the P21 parameter of Dershowitz and Herda [8]. The Monte Seco tunnel located in Espírito Santo, Brazil, case study was chosen to perform the flow analysis of mesh properties, thus verifying Reeves' method in a rock mass with discontinuities described by Baecher's model, which does not follow a power law [11]. It was possible to generate 200 three-dimensional models 20m x 20m x 20m of the rock mass using the UnblocksGen program [12]. A horizontal cut of the structural model was made to obtain the two-dimension mesh, figure 1.

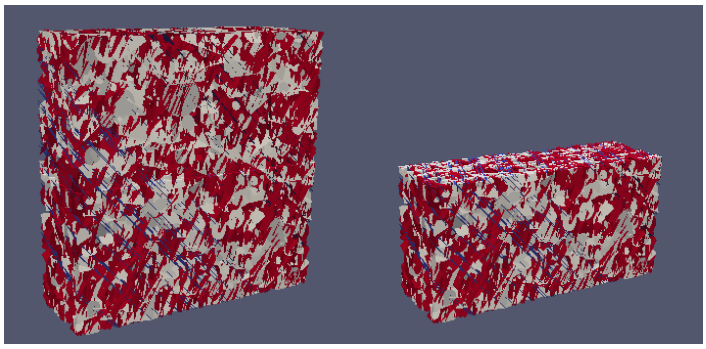

Fig. 1: Example of the intersection process with UnblocksGen.

The parameters of the sets of discontinuities for the Monte Seco tunnel were showed by Rasmussen et al. [11] and are listed as follows:

Table 1: Properties of the sets of discontinuities [11].

	Set 1	Set 2	Set 3
Model	Baecher	Baecher	Baecher
Dip direction (degrees)	110	180	258
Dip drive (degrees)	48	71	65
Fisher's constant (k)	50000	23	30
Probabilistic distribution	Deterministic	Lognormal	Lognormal
Persistence's mean (m)	200	1,45	2,04
Persistence's standard deviation (m)	0	1,04	0,89
P criteria	P10 = 1,2 m^{-1}	P32 = 1,24 m^2/ m^3	P 32 = 2,12 m^2/ m^3

The water flow was calculated considering the parallel plates hypothesis and the rock mass saturated the hydraulic aperture was considered uncorrelated with the discontinuities' length [5]. Based on the flow calculation, two types of discontinuities were defined in the same way as Reeves et al. [1]. These were the hydraulic backbone and the dominant discontinuities. The first aimed to restrict the discontinuities to those with at least some water flux. Therefore, it was specified for them that the mesh should have a minimum flow of 1 10-11 m3/s. The dominant discontinuities are those through which the water flux is higher. A limit is specified according to the following formula:

$$F_D \geq \frac{2G_F}{N_B} \tag{1}$$

Where,

F_D is the flow through a dominant discontinuity, G_F is the global water flux through the mesh and N_B is the number of backbone discontinuities at the boundary of the model.

Following Reeves' et al. [1] model, a first simulation was done considering the hydraulic aperture of all the discontinuities being equal to 5 10^{-4} m. After that, a second scenario was made attributing a lognormal distribution to the hydraulic aperture with the same mean as in the previous scenario and a standard deviation of 5 10^{-4} m. Then the mesh was scanned with a line crossing all the domain. The scanline was projected from the middle of the domain to the frontiers, then verified the intersections with all the three types of discontinuities and repeated the process rotating the scanline for every 5 degrees. The average distance of intersection was considered equal to the length of the scanline divided by the number of intersections.

4. Results

To obtain the discontinuities mesh, it was necessary to generate initially the three-dimensional model of the rock mass. For this, the Unblocksgen program was used and density criteria were inserted, table 1. A line mapping was used to insert discontinuities of the first set, until P10 was equal to 1.2 discontinuity/m. For set 2, the mapping was done in the volume with P32 equal to 1.24 m2/ m3 and for set 3 was P32 equal to 2.12 m2/ m3. After the generation of the three-dimensional model, the mesh is obtained by intersection of the 3D model with a horizontal plane. Constant gradient boundary conditions were entered. Thus, the program made it possible to calculate the water pressure at the nodes, water flow through the discontinuities, in addition to the classification of the types of discontinuities. In Figure 2, the results of the water pressure at the nodes, the hydraulic backbone and the dominant discontinuities for the Monte Seco tunnel are illustrated.

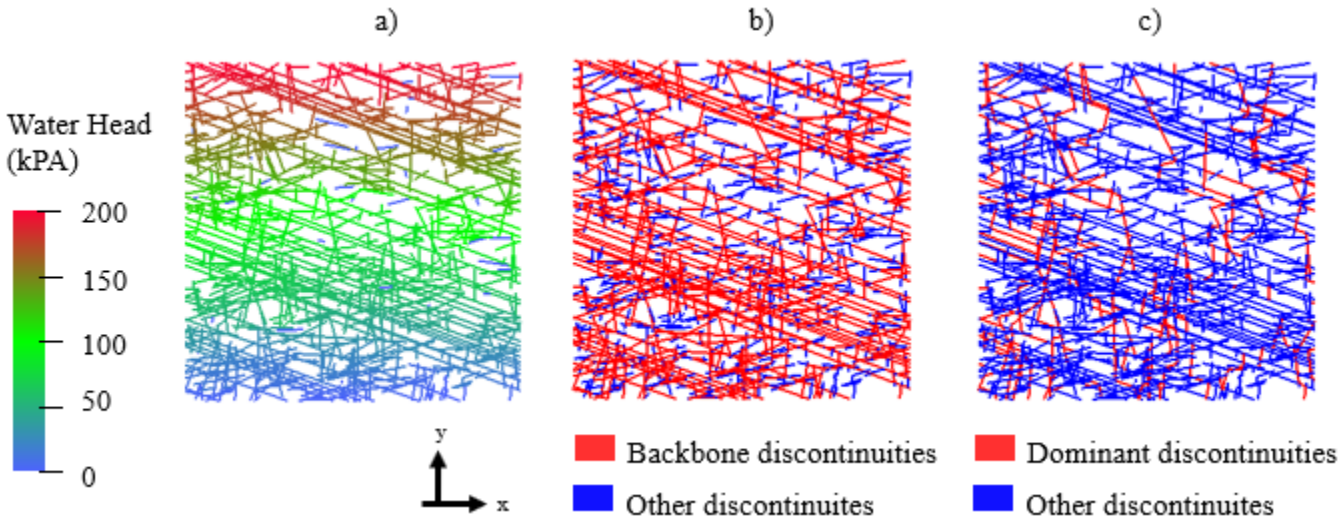

Fig. 2: Water flow through the discontinuities simulation: a) Water pressure at the nodes. b) Hydraulic backbones. c) Dominant discontinuities.

In Figure 2a, it was possible to observe the results for water pressure at the nodes. It showed an intensely fractured rock mass and fairly uniform reduction across the mesh. Some stretches at the top of the mesh were dark blue, which indicates that water pressure in these stretches is equal to zero; thus, they are not connected to the mesh. Figure 2b showed that most of the discontinuities displayed some water flow and were included in the hydraulic backbone. Most of the discontinuities that were not in the hydraulic backbone belonged to set 3 and were oriented in the direction of axis x. Figure 2c displayed a very different trend. Most of the discontinuities did not belong to the dominant discontinuities. There were far fewer discontinuities from the first set in this third group, but in some simulations they could play a greater role depending on the connectivity. The dominant discontinuities were composed mostly by the discontinuities of the second set, oriented in the y direction.

From the simulations, the values of output flow for each of the scenarios were also obtained. The results are shown in figure 3 below:

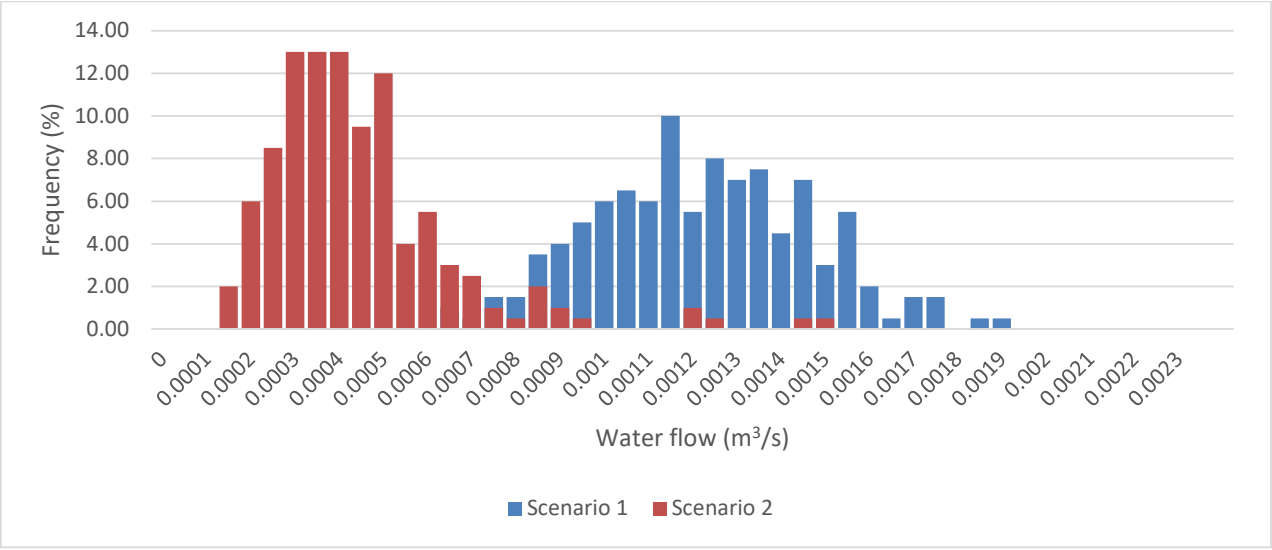

Fig. 3: Water flux through the mesh for the first and second scenarios.

For the first scenario, with the hydraulic aperture as a deterministic value, a mean value of 1,2 10-3m3/s was found for the water flow and a standard deviation of 6,2 10-4m3/s. For the second scenario, probabilistic values were assumed for the hydraulic aperture, a mean water flow equal to 4,4 10-4m3/s with a standard deviation of 1,1 10-4m3/s was found. Figure 3 showed that the water flow was normally smaller in the second scenario than in the first; furthermore, there was also a reduction in the coefficient of variation value from the first to the second scenario. The water flow seemed to follow a normal distribution in the first scenario, but a lognormal distribution in the second scenario.

By classifying the types of discontinuities and calculating the lengths, it was possible to obtain the relationship between the density of discontinuities and the water flow, figures 4 and 5.

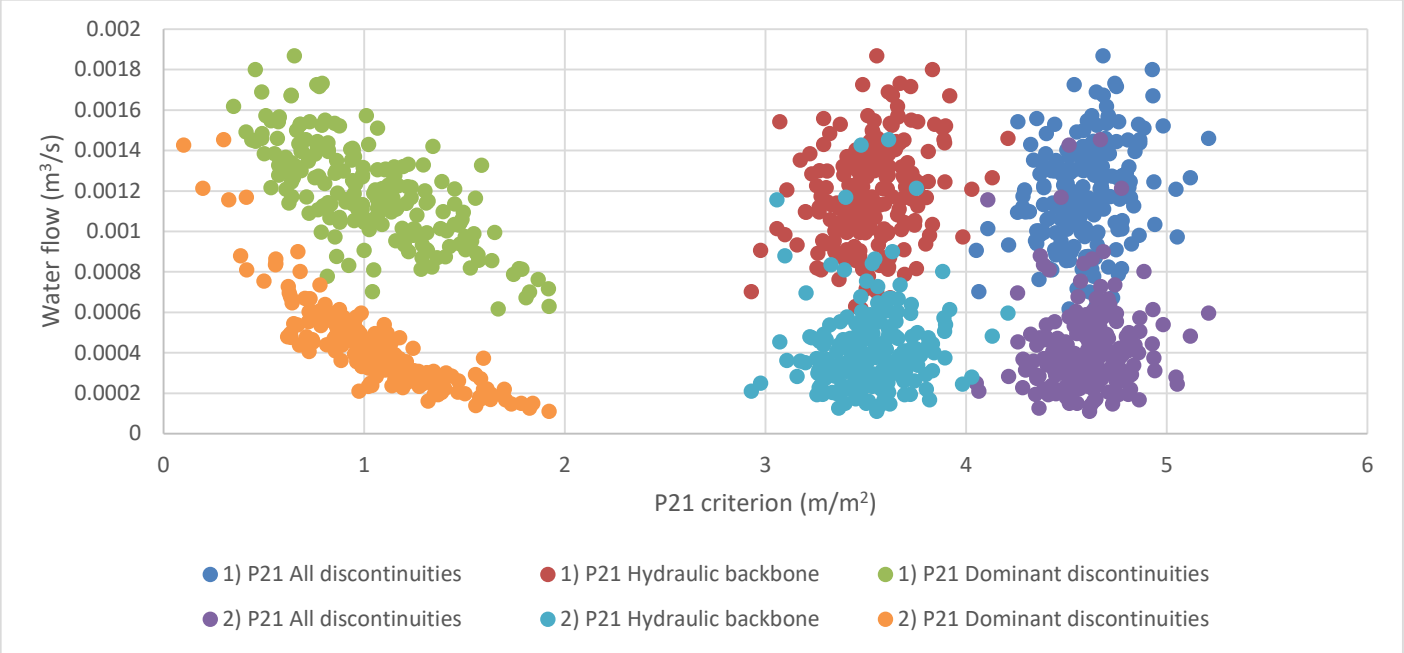

Figure 4: Relationship between water flux and the P21 criterion for every type of discontinuity in scenarios 1 and 2.

Figure 4 indicates a very similar behavior in both scenarios, the main difference being the intensity of the flow. It was not possible to observe any clear trend in the relationship between the density of all discontinuities and the water flow or between the hydraulic backbone and the water flow. For both types, the result is quite similar, with just a shift on the axis of P21. In both scenarios the mean and the standard deviation of P21 values for all discontinuities were equal to 4.60 and 0,18 m/m2, respectively. The hydraulic backbone also had very close P21 values of mean and standard deviations. They were equal to 3.53 and 0.19 m/m2, respectively. The water flow was normally bigger in the first scenario, with constant hydraulic aperture values, as observed by Reeves et al. [1]. The mean and the standard deviation of the water flow were of 1.2 10-3 and 2.5 10-4 m3/s in the first scenario and of 4.2 10-4 and 2.1 10-4 m3/s in the second. The dominant discontinuities, however, exhibited a considerably different behavior. Although they are in the same flow range, the variation of P21 is much more significant, from 0,10 m/m2 to 1,92 m/m2, in the second scenario. Furthermore, they showed an inversely proportional trend between the water flux and the dominant discontinuities' density. In the second scenario, there was a simulation with a much higher flux value equal to 4.6 10-3 m3/s and very small P21 dominant discontinuity value, 0,035 m/m2, probably due to a high conductive discontinuity at the edge of the model. For this reason, this simulation was not considered in this analysis.

Next, the scanning method by Reeves et al. [1] was applied and the following results were obtained:

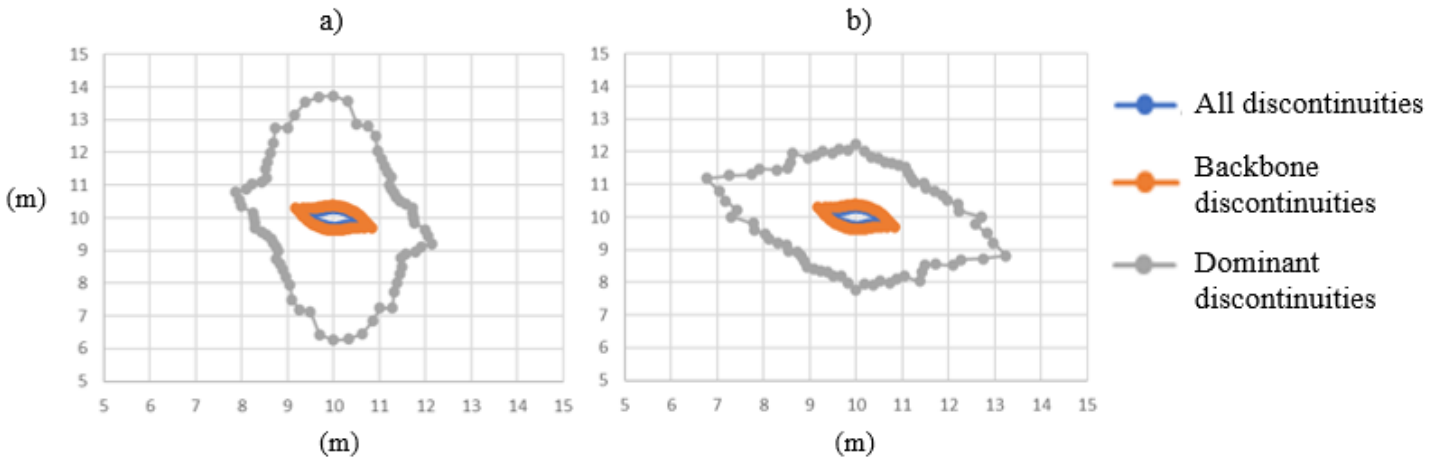

Fig. 5: Mean of the scanlines directional distances with all the three types of discontinuities for: a) scenario 1 e b) scenario2.

Figure 5 showed very similar results for scenario 1 and scenario 2 for all discontinuities and the hydraulic backbone. The graphic obtained was also similar for the dominant discontinuities in the second scenario with variable aperture, although with higher mean distance. In the first scenario with constant hydraulic aperture, the mean distance displayed much higher values in the y direction for the dominant discontinuities. The smallest distances were observed for the group of all discontinuities, followed by the hydraulic backbone and then the dominant discontinuities. The difference between the hydraulic backbone and all discontinuities is not very significant, while the difference is greater between the dominant discontinuities and the hydraulic backbone. Except for the dominant discontinuities in the first scenario, the three scans have a similar format. The shape is rounded and shorter distances for angle values between 45 and 135 degrees and between 225 and 315 dergees. For the other orientations, the shape is sharper and the distances are much greater.

5. Discussion

As can be seen in figure 2, the rock mass of the Monte Seco tunnel is intensely fractured. It played an important role in the connectivity of the discontinuities and in the formation of the extensive hydraulic backbone as shown in figure 2b. The large number of discontinuities that constitute the hydraulic backbone indicated the possibility for the water flow to adopt different paths. Furthermore, the discontinuities of set 1 stood out in the formation of these paths. This was due to the high persistence of these discontinuities, which favored their connection with those of other sets. Thus, three main ranges of hydraulic backbone were identified, where discontinuities of set 1 may be found. Along these ranges, the presence of other sets in the hydraulic backbone group was also more noticeable. Outside the range, the spacing between the hydraulic backbone was greater. Set 3 of discontinuities, although well connected, had the most discontinuities not belonging to the hydraulic backbone. This was due to its orientation towards the x axis and the boundary conditions that favored water flow in the y direction. This trend is even clearer for the dominant discontinuities in figure 3c. In this case, almost all dominant discontinuities belonged to set 2 and are mostly oriented towards the y axis.

As expected from the results of Reeves et al [1], scenario 1 with invariant hydraulic aperture presented a higher water flow than the scenario 2, figure 3. The standard deviation of the water flux in the first scenario is still a little higher than the one of the second scenario, but the coefficient of variability in the second scenario increased considerably. A possible explanation for this observation is that the variability of the mesh alters the connectivity and the flow paths. Variable conductance together with the availability of several paths made certain stretches less accessible but contributed to others. Furthermore, the variability of the hydraulic aperture impacted significantly the water flow, since it changed the water flow distribution. In the first scenario, it seemed more like a normal distribution and in the second more like a lognormal, the same as the hydraulic aperture. However, the reduction in permeability, by inserting variability in the conductance parameter, is still the most significant consequence, as the mean flow rate was reduced by 63.3%.

When comparing the water flow with the density of total discontinuities and with the hydraulic backbone, it was not possible to verify any clear relationship between them, figure 4. However, quite dispersed values were observed in both scenarios. As the meshes were created with the same geometric criteria with orientations and persistence being the only variables, the oscillation of the results must be related to the change in the mesh's connectivity. In comparison with the total of discontinuities and with the hydraulic backbone, the dominant discontinuities stood out due to their large variability and apparently inversely proportional relationship with the flow. The amplitude is significant with P21 values ranging from close to 0 m/m2 in scenario 2, up to practically 2 m/m2 for both scenarios. In the context of an extensive hydraulic backbone and the criterion used to classify a discontinuity as dominant, if there is little flow variation across the hydraulic backbone, it is natural that small changes in criteria values could generate large changes in the number of discontinuities classified as dominant. Thus, smaller flow values would generate a lower classification threshold in dominant discontinuity, so more discontinuities could be included, which would increase the P21 value. Furthermore, the formation of preferential flow paths may have increased the water flow through specific discontinuities, which elevated the limit criterion and reduced P21 dominant discontinuities. Although it was not observed in this study, a relationship between the flow and the P criteria of Dershowitz and Herda [8] should not be discarded. This should be observed when the mesh is generated; for this study it would be the P32 criteria for mesh formation and not necessarily in the simulation with statistical distribution of orientations.

The results obtained for the mean directional distances, figure 5, with the scanline were very similar in both scenarios for the backbone discontinuities and all discontinuities. The dominant discontinuities in the second scenario showed the same trend, but with higher distances, figure 5b. One reason for this observation was the intensity of fracturing of the rock mass, which can also be seen in figures 2a and 2b, that created an extensive hydraulic backbone. This highlights the possibility of water flow over a large part of the mesh. The maximum value of the mean fracture distance found was equal to 0.56 for all discontinuities in an area of 20 by 20 m. For the dominant discontinuities, the value increased to a maximum of 2.50 m parallel to set 1 in scenario 1. The shape of the figure observed was strongly influenced by the orientation of the sets of discontinuities. The highest values observed are precisely in the orientation parallel to set 1 of discontinuities for all types of discontinuities. This again shows that they played an important role in forming and conducting flow paths. The acute shape of the figure in this region was given by the meeting of sets of discontinuities 2 and 3. The smaller distances to the other angles was due to the greater number of discontinuities that encompassed discontinuities of sets 1, 2 and 3. The circular region may be due to a more pronounced randomness effect, as observed by Reeves et al. [1]. The difference of approximately 90 degrees between sets 2 and 3, with low Fisher constant values, may have contributed to this. In figure 5a, the directional distances for the dominant discontinuities in the first scenarios had a very different shape with higher distances in the y direction. This is due to some simulations in which the flow paths were predominantly in the y direction, therefore it was less probable to intersect dominant discontinuities in this direction. However, this was not observed in the second scenario, figure 5b, with variable hydraulic aperture which, together with high connectivity, seemed to facilitate flow in other directions. As the hydraulic backbone and second scenario’s dominant discontinuities suggest; the high values for the distance in the y axis may be a irregularity. The insertion of the drain would change the boundary conditions, therefore the drain length could be smaller. Thus, the previous direction could be the recommended orientation to ensure the greatest number of intersections of discontinuities with shorter drains.

6. Conclusion

Many properties of the discontinuities affect the water flux through the fractured rock mass. Most of the time, however, hard to determine them precisely. Therefore, many uncertainties are present in the assessment of the water flux. The objective of this work was conducted to identify the effect of the most important properties on the water flux, as well as to identify the best orientation for a drainage system, based on a case study of the fractured rock mass of a tunnel in Brazil. The connectivity of discontinuities proved to be an essential factor for water flow. Because of it, the rock mass presented an extensive hydraulic backbone, thus providing several possibilities for water flow. An important factor was the presence of discontinuities set 1, which had infinite persistence and enabled the connection between the various discontinuities. Water flow was also impacted by the various simulations with different meshes, that is, by the variation in connectivity, and by the variability of the hydraulic aperture, as a reducing element. The lack of relationship between P21 and water flow indicated that, for a given

mesh with variable discontinuity orientations, water flow is more impacted by the connectivity between the discontinuities than by the intensity of fracturation. However, the latter should still be important when it comes to the criteria for modeling the fractured rock mass. In addition, it was possible to identify which regions of the rock mass had higher degrees of fracture intensity and which would be the best direction for the insertion of drains.

Acknowledgements

The authors would like to acknowledge the financial support granted by the Coordenação de Aperfeiçoamento de Pessoal de Nível Superior - Brasil (CAPES).

References

[1] D. M. Reeves, R. Parashar, G. Pohll, R. Caroll, T. Badger and K. Willoughby "The use of discrete fracture networks simulations in the design of horizontal hillslope drainage networks in fractured rock," *Eng. Geology*, vol. 163, pp. 132-145, 2013.

[2] E. Karimzade, M. Sharifzadeh, H. R. Zarei, K. Shahriar, and M. Cheraghi Seifabad, "Prediction of water inflow into underground excavations in fractured rocks using a 3d discrete fracture network (dfn) model," *Arab J. of Geosci*, vol. 10, no. 9, 2017.

[3] I. Vazaios, M. Diederichs and N. Vlachopoulos, " DFN generation for mechanical stability analysis of underground works," *Proceedings of the ITA WTC 2015 Congress and 41st General Assembly*, Dubrovnik, Croatia, 2015,pp. 1-11.

[4] M. Javadi, M. Sharifzadeh, and K. Shahriar, "Uncertainty analysis of groundwater inflow into underground excavations by stochastic discontinuum method: case study of siah bisheh pumped storage project, Iran," *Tunn. Undergr. Sp. Technol.*, vol. 51, pp. 424-438, 2016.

[5] S. D. Priest, *Discontinuity Analysis for Rock Engineering*. London, UK: Chapman & Hall, 1993.

[6] W. S. Dershowitz and H. H. Einstein, "Characterizing rock joint geometry with joint system models," *Rock Mech. Rock Eng.*, vol. 21, no. 1, pp. 21-51, 1988.

[7] W. Zhu, S. Khirevich and T. W. Patzek, (2021) Impact of fracture geometry and topology on the connectivity and flow properties of stochastic fracture networks [Online]. Available: https://agupubs.onlinelibrary.wiley.com/doi/10.1029/2020WR028652

[8] W. S. Dershowitz and H. H. Herda, "Interpretation of fracture spacing and intensity," *Paper presented at the 33rd US Symposium on Rock Mechanics*, Santa Fé, NM, 1992, 1992.

[9] D. C. Wyllie and C. W. Mah, *Rock Slope Engineering: Civil and Minnig*. Taylor and Francis, 2005.

[10] L. E. Widodo, T. A. Cahyadi, Z. Syihab, S. Notosiswoyo, I. Iskandar, H. C. Rustamaji, "Development of drain hole design optimisation: a conceptual model for open pit mine slope drainage system with fractured media using a multi-stage genetic algorithm," *Environ. Earth Sci.*, vol. 77, 2018.

[11] L. L. Rasmussen, P. P. Cacciari, M. M. Futai, M. M. de Farias, A. P. de Assis, "Efficient 3D probabilistic stability analysis of rock tunnels using a Lattice model and cloud computing," *Tunn. Undergr. Sp. Technol.*, vol. 85, pp. 282-293, 2019.

[12] L. L. Rasmussen, "UnBlocksgen: a python library for 3d rock mass generation and analysis," *SoftwareX*, vol. 12, 2020.